REPORT 930

AN ANALYTICAL METHOD OF ESTIMATING TURBINE PERFORMANCE

By Fred D. Kochendorfer and J. Cary Nettles

SUMMARY

A method is developed by which the performance of a turbine over a range of operating conditions can be analytically estimated from the blade angles and flow areas. In order to use the method, certain coefficients that determine the weight flow and the friction losses must be approximated.

The method is used to calculate the performance of the single-stage turbine of a commercial aircraft gas-turbine engine and the calculated performance is compared with the performance indicated by experimental data. For the turbine of the typical example, the assumed pressure losses and the turning angles give a calculated performance that represents the trends of the experimental performance with reasonable accuracy. The exact agreement between analytical performance and experimental performance is contingent upon the proper selection of a blading-loss parameter.

INTRODUCTION

The analytical determination of the performance of a gas-turbine engine under various operating conditions or the prediction of engine performance at other-than-design conditions requires a knowledge of the complete performance of each of the engine components, especially of the compressor and the turbine (references 1 and 2). Knowledge of the component performance characteristics that can be obtained from jet-propulsion-engine investigations is necessarily limited and does not, in general, provide a solution to the problem of component matching. A performance test of a compressor or a turbine as a single unit provides all the necessary information, but such testing of high-speed high-capacity units requires costly auxiliary equipment. An analysis that can be used either with or without engine data to estimate compressor and turbine performance would be valuable. An analytical method for estimating turbine performance from the blade angles and flow areas was therefore developed at the NACA Lewis laboratory in 1947 and is described herein.

The most important prerequisite for analysis of turbine performance is a knowledge of the flow angles and the pressure losses of the turbine blades and of the variations of these quantities with changes in angle of incidence and in entrance Mach number. References 3 to 5 present turning angles and losses of typical turbine blades, but their results cannot be generalized to the extent required to obtain the performance of a given blade profile. For the turbine analysis, the turning angles, the pressure losses, and their variations with entrance and exit conditions are assumed, the assumptions being consistent with the information in references 3 to 5. The performance of a turbine of a commercial aircraft gas-turbine engine is determined by the analytical method and the results are compared with experimental data.

SYMBOLS

The following symbols and abbreviations are used in this analysis:

A	area perpendicular to velocity, (sq ft)
a, b	blading-loss functions
C	discharge coefficient
D	pitch-line diameter of turbine, (ft)
g	acceleration due to gravity, 32.2 (ft/sec^2)
hp	horsepower
i	angle of incidence (angle between direction of approaching fluid and tangent to camber line), (deg)
K	blading-loss parameter
P	total pressure, (lb/sq ft)
p	static pressure, (lb/sq ft)
R	gas constant, 53.3 (ft-lb/(°F)(lb))
r_i	inlet velocity ratio, $\left[\frac{U/\sqrt{\theta_{1,s}}}{(V_{3,s}/\sqrt{\theta_{1,s}})\sin\alpha_{f,s}}\right]$
r_o	outlet velocity ratio, $\left[\frac{U/\sqrt{\theta_{1,s}}}{(V_{6,r}/\sqrt{\theta_{1,s}})\sin\sigma_f}\right]$
T	total temperature, (°R)
t	static temperature, (°R)
U	rotor-pitch-line velocity, (ft/sec)
V	fluid velocity, (ft/sec)
W	weight flow, (lb/sec)
X	pressure-ratio function, $\left[(p/P)^{\frac{2}{\gamma}}-(p/P)^{\frac{\gamma+1}{\gamma}}\right]^{\frac{1}{2}}$
x, y	jet-deflection parameters
α	stator-blade exit angle at pitch line measured from axial plane, (deg)
$\alpha_{f,r}$	angle between fluid velocity relative to rotor and axial plane at inlet to rotor, (deg)
$\alpha_{f,s}$	angle between fluid absolute velocity and axial plane at exit from stator, (deg)
β	rotor-blade entrance angle at pitch line measured from axial plane, (deg)
γ	ratio of specific heats
δ	ratio of absolute total pressure to static pressure of NACA standard atmosphere at sea level
θ	ratio of absolute total temperature to static temperature of NACA standard atmosphere at sea level

924778—51——14

ϵ angle between fluid absolute velocity and axial plane at exit from turbine, (deg)
η_{ad} adiabatic efficiency
ν angle of jet deflection, (deg)
ρ mass density, (slugs/cu ft)
σ rotor-blade exit angle at pitch line measured from axial plane, (deg)
σ_f angle between fluid velocity relative to rotor and axial plane at exit from rotor, (deg)

Subscripts:
a before cascade
b at entrance to cascade
c after cascade
r with respect to rotor
s with respect to stator
0 ambient (NACA standard atmosphere at sea level)
1 stator inlet at pitch line
2 stator throat at pitch line
3 stator outlet at pitch line
4 rotor inlet at pitch line
5 rotor throat at pitch line
6 rotor outlet at pitch line

ANALYSIS

STATEMENT OF PROBLEM

The quantities that can be employed to define the turbine performance and the independent or operating variables are as follows:

Dependent variables	*Independent variables*
Total-pressure ratio, P_1/P_6	Inlet total pressure, P_1
Total-temperature ratio, T_1/T_6	Inlet total temperature, T_1
Weight flow, W	Rotor-pitch-line velocity, U
Horsepower, hp	Outlet static pressure, p_6
Adiabatic efficiency, η_{ad}	

By dimensional analyses or by a method similar to that used in the analysis which follows, the four independent variables can be reduced to two independent parameters. The dependent and independent parameters would then be as follows:

Dependent parameters	*Independent parameters*
Total-pressure ratio, $P_{1,s}/P_{6,s}$ (based on axial leaving velocity)	Turbine pressure ratio, $P_{1,s}/p_6$
Total-temperature ratio, $(T_{1,s}-T_{6,s})/T_{1,s}$	Rotor-pitch-line velocity, $U/\sqrt{\theta_{1,s}}$
Weight flow, $(W\sqrt{\theta_{1,s}})/\delta_{1,s}$	
Horsepower, $\mathrm{hp}/(\sqrt{\theta_{1,s}}\delta_{1,s})$	
Adiabatic efficiency, η_{ad}	

The object of this analysis is to determine the value of each of the dependent parameters for given values of the two independent parameters.

OUTLINE OF METHOD

In the analysis, the turbine pressure ratio $P_{1,s}/p_6$ cannot be used directly because it is a product of the interdependent pressure ratios $P_{1,s}/P_{3,s}$, $P_{3,s}/p_3$, $p_3/P_{4,r}$, $P_{4,r}/P_{6,r}$, and $P_{6,r}/p_6$, which cannot be determined for a given value of $P_{1,s}/p_6$. If instead, values are chosen for $P_{3,s}/p_3$ and $U/\sqrt{\theta_{1,s}}$, and if the pressure losses and the turning angles are known or assumed, a step-by-step process can be employed in which the successive pressures, temperatures, and velocities can be calculated from the principles of fluid mechanics. After the pressures, the temperatures, and the velocities at the turbine outlet have been obtained, the performance parameters and also $P_{1,s}/p_6$ can be computed; the performance parameters can then be plotted as functions of $P_{1,s}/p_6$ and $U/\sqrt{\theta_{1,s}}$.

ASSUMPTIONS

Blading losses.—The loss in total pressure that occurs during passage of fluid through a cascade of blades may, for convenience of analysis, be separated into two losses: the entry loss caused by other-than-zero entrance angle, and the friction loss that results from the actual passage through the cascade.

The entry loss can be approximated (fig. 1) by resolving the entering velocity into components normal and parallel

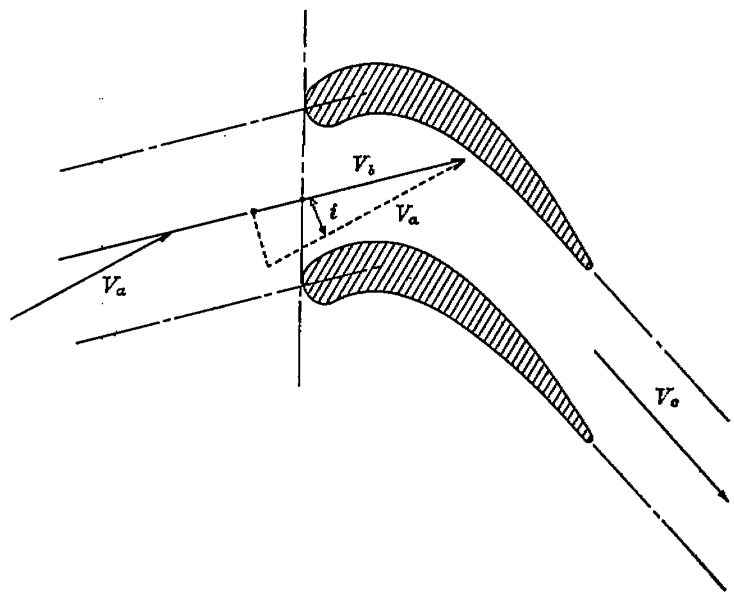

FIGURE 1.—Blading-loss diagram.

to the blade-entrance direction and by then assuming that the normal component is lost; that is, $V_b = V_a \cos i$. This approximation gives entry losses that are independent of the sign of the angle of incidence. Actually, the losses for positive angles are greater than the losses for corresponding negative angles, but for blading having a solidity greater than 1.5 the error is probably not too large. For blades having solidities less than 1.0, however, a better approximation might be obtained by assuming the normal component to be lost for positive angles of incidence and no entry losses to occur for negative angles.

The friction loss can be approximated by

$$\Delta P_{loss} = \frac{2(\gamma-1)}{\gamma} K\left(\frac{1}{2}\rho V^2\right)$$

where, for a particular cascade, K is considered to be a constant that accounts for all the loss in total pressure occurring across the cascade when the fluid enters at zero entrance angle. The quantity $\frac{1}{2}\rho V^2$ is the average dynamic head of the fluid in the cascade. This expression for loss (appendix A) can be rewritten as follows:

For the stator,

$$P_{3,s}=P_{1,s}\frac{1}{b_3} \tag{1}$$

For the rotor,

$$P_{6,r}=P_{4,r}\frac{a_4}{b_6} \tag{2}$$

where

$$a=1-K\left(\frac{p}{P}\right)^{\frac{1}{\gamma}}\left[1-\left(\frac{p}{P}\right)^{\frac{\gamma-1}{\gamma}}\right]$$

and

$$b=1+K\left(\frac{p}{P}\right)^{\frac{1}{\gamma}}\left[1-\left(\frac{p}{P}\right)^{\frac{\gamma-1}{\gamma}}\right]$$

A plot of a and b as functions of p/P for various values of K when γ equals 1.34 is given in figure 2.

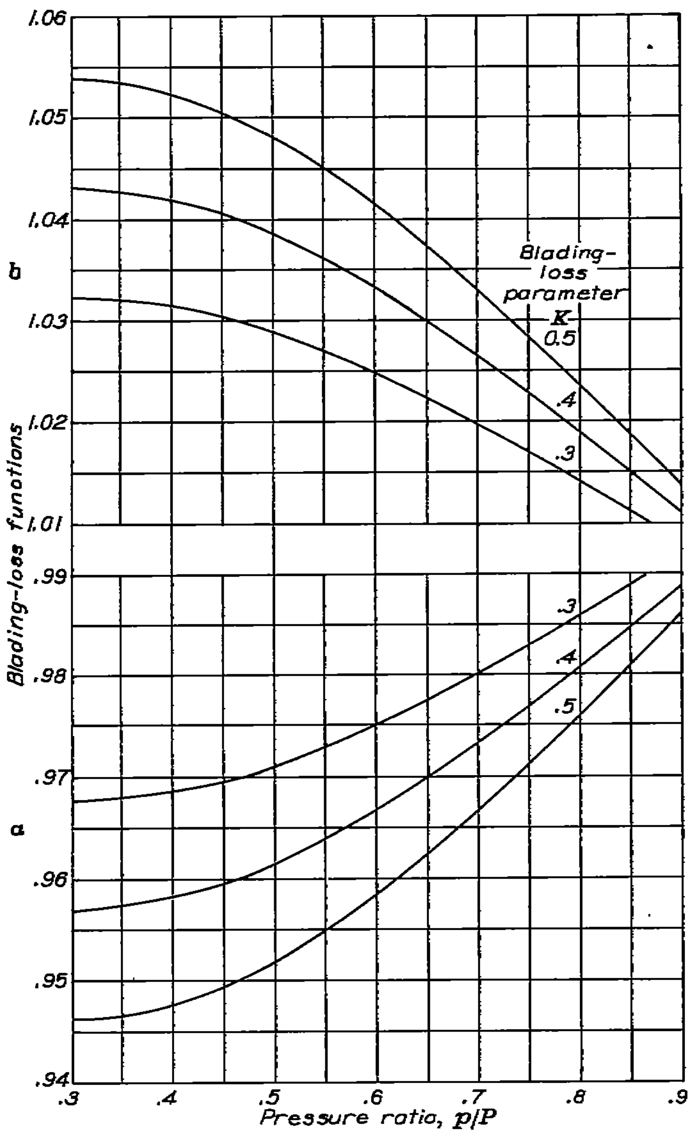

FIGURE 2.—Variation of blading-loss functions with ratio of static to total pressure for severa values of blading-loss parameter. γ, 1.34.

Other losses such as blade-tip and separation losses should be small for well-designed turbines operating reasonably close to design conditions and therefore will be neglected in this analysis.

Turning angles.—The angle through which a fluid is turned on passing through a given cascade depends on the angle of incidence, the blade exit angle, and the entrance Mach number. For blading having a solidity of 1.5 or greater, the turning angle so varies with the angle of incidence that the fluid exit angle remains approximately equal to the blade exit angle. The effect of entrance Mach number on the exit angle is small unless sonic velocity exists at the blade throat. In this case, the jet of fluid passes the trailing edge of the blade at a sonic or supersonic velocity and, if the pressure in the region beyond the cascade is not equal to the pressure at the blade throat, the jet will deflect. The angle of deflection is assumed to depend on the pressure ratio in accordance with the Prandtl-Meyer theory. (See, for example, reference 6.) Although a deflection may actually occur at both the upper and lower trailing edges and the flow configuration may be quite complex, for simplicity the mean deflection given by the Prandtl-Meyer theory is assumed. The angle of jet deflection as a function of the ratio of static to total pressure in the region beyond the trailing edge of the blade for sonic throat velocity is calculated from the relations in appendix B and is plotted in figure 3. The angle at which the fluid leaves the blade is

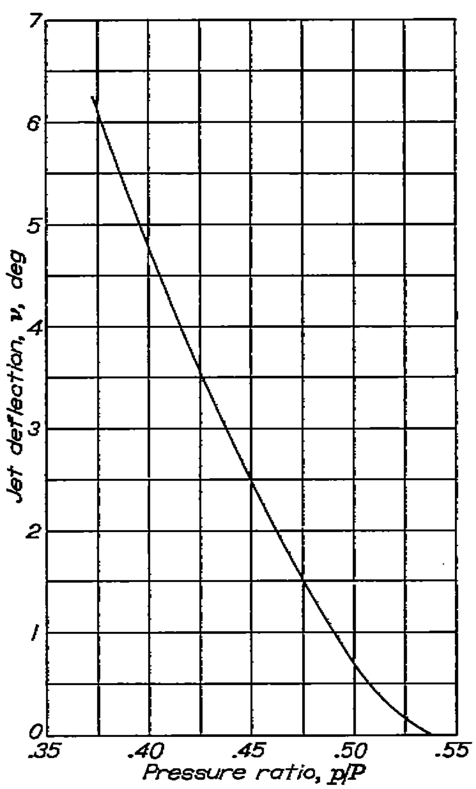

FIGURE 3.—Variation of jet deflection with ratio of static to total pressure in region beyond blade exit for assumed Prandtl-Meyer flow. γ, 1.34.

therefore assumed equal to the difference between the geometrical angle at the pitch line of the trailing edge of the blade and the angle of jet deflection given by the Prandtl-Meyer theory.

BASIC EQUATIONS

The basic equations can be derived from the definition of total pressure

$$P=p\left[1+\frac{(\gamma-1)V^2}{2\gamma gRt}\right]^{\frac{\gamma}{\gamma-1}} \tag{3}$$

the definition of total temperature

$$T=t\left[1+\frac{(\gamma-1)V^2}{2\gamma gRt}\right] \tag{4}$$

and the equation of state

$$p=\rho gRt \tag{5}$$

Equations (3) and (4) can be rewritten as

$$p=P\left[1-\frac{(\gamma-1)V^2}{2\gamma gRT}\right]^{\frac{\gamma}{\gamma-1}} \tag{6}$$

and

$$t=T\left[1-\frac{(\gamma-1)V^2}{2\gamma gRT}\right] \tag{7}$$

The weight flow at any point is $W=Cg\rho AV$ and from equations (5) to (7)

$$\rho=\frac{p}{gRt}=\frac{p}{gRT\left[1-\frac{(\gamma-1)V^2}{2\gamma gRT}\right]}=\frac{p}{gRT}\left(\frac{P}{p}\right)^{\frac{\gamma-1}{\gamma}}$$

Also from equation (6)

$$V^2=\frac{2\gamma gR}{\gamma-1}T\left[1-\left(\frac{p}{P}\right)^{\frac{\gamma-1}{\gamma}}\right] \tag{8}$$

so that

$$W=CA\frac{p}{RT}\left(\frac{P}{p}\right)^{\frac{\gamma-1}{\gamma}}\sqrt{\frac{2\gamma gRT}{\gamma-1}}\left[1-\left(\frac{p}{P}\right)^{\frac{\gamma-1}{\gamma}}\right]^{\frac{1}{2}}$$

or

$$W=CA\sqrt{\frac{2\gamma g}{(\gamma-1)R}}\frac{P}{\sqrt{T}}\left[\left(\frac{p}{P}\right)^{\frac{2}{\gamma}}-\left(\frac{p}{P}\right)^{\frac{\gamma+1}{\gamma}}\right]^{\frac{1}{2}} \tag{9}$$

TURBINE ANALYSIS

The analysis is made for a single-stage partial-reaction turbine having one set of stator blades and one set of rotor blades, each of the blade sets forming a series of convergent nozzles. A schematic diagram of the turbine is shown in figure 4 and the velocity diagram in figure 5.

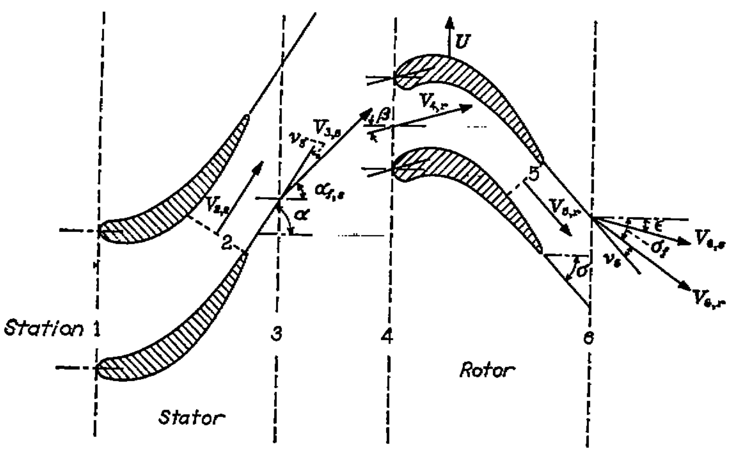

FIGURE 4.—Schematic diagram of turbine.

The quantities obtained from the geometry of the turbine are:

Area of stator throat, A_2
Area of rotor throat, A_5

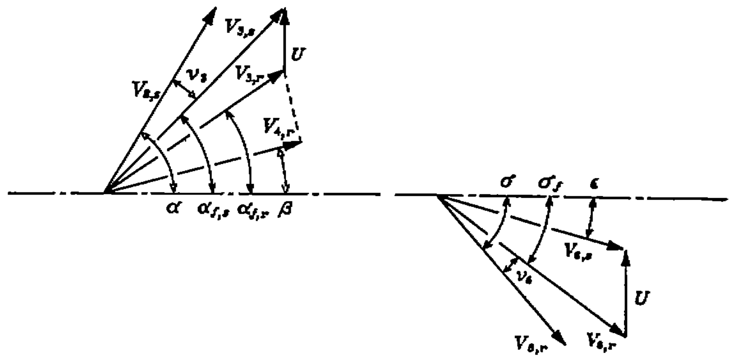

FIGURE 5.—Turbine-velocity diagram.

Pitch-line diameter of turbine, D
Stator-blade exit angle, α
Rotor-blade entrance angle, β
Rotor-blade exit angle, σ

The quantities that must in general be assumed are:

Discharge coefficient, C
Blading-loss parameter, K
Ratio of specific heats, γ

Stator.—When a value for $p_3/P_{3,s}$ is assumed, then b_3 can be obtained from figure 2 and hence $p_3/P_{1,s}$ can be calculated from equation (1),

$$\frac{p_3}{P_{1,s}}=\frac{p_3}{P_{3,s}}\frac{1}{b_3}$$

The weight of gas flowing through the stator, from equation (9), is

$$W=CA_2\sqrt{\frac{2\gamma g}{(\gamma-1)R}}\frac{P_{2,s}}{\sqrt{T_{2,s}}}X_{2,s} \tag{10}$$

where

$$X_{2,s}=\left[\left(\frac{p_{2,s}}{P_{2,s}}\right)^{\frac{2}{\gamma}}-\left(\frac{p_{2,s}}{P_{2,s}}\right)^{\frac{\gamma+1}{\gamma}}\right]^{\frac{1}{2}}$$

In figure 6, X is shown as a function of p/P for two values of γ. If $\frac{p_3}{P_{3,s}}\leq\left(\frac{2}{\gamma+1}\right)^{\frac{\gamma}{\gamma-1}}$, the stator is choked and $\frac{p_2}{P_{2,s}}=\left(\frac{2}{\gamma+1}\right)^{\frac{\gamma}{\gamma-1}}$. Inasmuch as $P_{1,s}=P_{2,s}b_2$ and $T_{1,s}=T_{2,s}$, the weight-flow parameter from equation (10) becomes

$$\frac{W\sqrt{\theta_{1,s}}}{\delta_{1,s}}=\frac{CA_2P_0}{\sqrt{T_0}b_2}\sqrt{\frac{2\gamma g}{(\gamma-1)R}}\left[\left(\frac{2}{\gamma+1}\right)^{\frac{2}{\gamma-1}}-\left(\frac{2}{\gamma+1}\right)^{\frac{\gamma+1}{\gamma-1}}\right]^{\frac{1}{2}} \tag{11}$$

If $\frac{p_3}{P_{3,s}}>\left(\frac{2}{\gamma+1}\right)^{\frac{\gamma}{\gamma-1}}$, then $P_{3,s}=P_{2,s}$ and $p_3=p_2$. Then $P_{1,s}=P_{2,s}b_2=P_{3,s}b_3$ and $T_{1,s}=T_{2,s}=T_{3,s}$; the weight-flow parameter then is

$$\frac{W\sqrt{\theta_{1,s}}}{\delta_{1,s}}=\frac{CA_2P_0}{\sqrt{T_0}b_3}\sqrt{\frac{2\gamma g}{(\gamma-1)R}}X_3 \tag{12}$$

The velocity leaving the stator, from equation (8), is given by

$$\frac{V_{3,s}}{\sqrt{\theta_{1,s}}}=\sqrt{T_0}\sqrt{\frac{2\gamma gR}{\gamma-1}}\left[1-\left(\frac{p_3}{P_{3,s}}\right)^{\frac{\gamma-1}{\gamma}}\right]^{\frac{1}{2}} \tag{13}$$

If the pressure ratio across the stator is supercritical, the deflection of the jet ν_3 as it leaves the stator can be obtained from figure 3 for $p_3/P_{3,s}$. The angle at which the jet leaves the stator is then $\alpha_{f,s}=\alpha-\nu_3$.

Rotor.—With an assumed value for $U/\sqrt{\theta_{1,s}}$

$$r_t=\frac{U/\sqrt{\theta_{1,s}}}{(V_{3,s}/\sqrt{\theta_{1,s}})\sin\alpha_{f,s}} \tag{14}$$

From the velocity diagram of figure 5

$$V_{3,r}^2=(V_{3,s}\sin\alpha_{f,s}-U)^2+(V_{3,s}\cos\alpha_{f,s})^2=(V_{3,s}\sin\alpha_{f,s})^2\left[\cot^2\alpha_{f,s}+(1-r_t)^2\right] \tag{15}$$

and

$$\tan\alpha_{f,r}=\frac{V_{3,s}\sin\alpha_{f,s}-U}{V_{3,s}\cos\alpha_{f,s}}=\tan\alpha_{f,s}\,(1-r_t) \tag{16}$$

According to the assumption on entry losses,

$$V_{4,r}=V_{3,r}\cos(\alpha_{f,r}-\beta)$$

With equation (15) and the expanded form of $\cos(\alpha_{f,r}-\beta)$, the preceding equation becomes

$$V_{4,r}=V_{3,s}\sin\alpha_{f,s}\left[\cot^2\alpha_{f,s}+(1-r_t)^2\right]^{\frac{1}{2}}(\cos\alpha_{f,r}\cos\beta+\sin\alpha_{f,r}\sin\beta)$$

or

$$V_{4,r}=V_{3,s}\sin\alpha_{f,s}\left[\cot^2\alpha_{f,s}+(1-r_t)^2\right]^{\frac{1}{2}}\cos\alpha_{f,r}(\cos\beta+\tan\alpha_{f,r}\sin\beta)$$

Also

$$\cos\alpha_{f,r}=\left(\frac{1}{1+\tan^2\alpha_{f,r}}\right)^{\frac{1}{2}}$$

so that finally by use of equation (16)

$$\frac{V_{4,r}}{\sqrt{\theta_{1,s}}}=\frac{V_{3,s}}{\sqrt{\theta_{1,s}}}\cos\alpha_{f,s}\left[\cos\beta+(1-r_t)\tan\alpha_{f,s}\sin\beta\right] \tag{17}$$

In order to find the total temperature with respect to the rotor, use of equation (4) gives

$$T_{1,s}=T_{3,s}=t_3+\frac{(\gamma-1)V_{3,s}^2}{2\gamma gR}$$

and

$$T_{3,r}=t_3+\frac{(\gamma-1)V_{3,r}^2}{2\gamma gR}$$

Therefore

$$T_{3,r}=T_{1,s}\left[1-\frac{(\gamma-1)(V_{3,s}^2-V_{3,r}^2)}{2\gamma gRT_{1,s}}\right]$$

and with equations (15) and (14)

$$\frac{T_{3,r}}{T_{1,s}}=1-\frac{\gamma-1}{2\gamma gRT_0}\left(\frac{U}{\sqrt{\theta_{1,s}}}\right)^2\left(\frac{2-r_t}{r_t}\right) \tag{18}$$

Use of equations (3) and (7) to find the total pressure at the entrance to the rotor with respect to the rotor gives

$$P_{4,r}=p_4\left[1+\frac{(\gamma-1)V_{4,r}^2}{2\gamma gRt_4}\right]^{\frac{\gamma}{\gamma-1}}$$

and

$$t_4=T_{4,r}-\frac{(\gamma-1)V_{4,r}^2}{2\gamma gR}$$

Then, because $T_{4,r}=T_{3,r}$ and because it is assumed that $p_4=p_3$, the pressure ratio at the rotor inlet is

$$\frac{p_3}{P_{4,r}}=\left[1-\left(\frac{V_{4,r}}{\sqrt{\theta_{1,s}}}\right)^2\left(\frac{\sqrt{\theta_{1,s}}}{\sqrt{T_{3,r}}}\right)^2\frac{\gamma-1}{2\gamma gR}\right]^{\frac{\gamma}{\gamma-1}} \tag{19}$$

The weight-flow parameter at the rotor throat can be written as

$$\frac{W\sqrt{\theta_{5,r}}}{\delta_{5,r}}=\frac{W\sqrt{\theta_{1,s}}}{\delta_{1,s}}\left(\frac{T_{3,r}}{T_{1,s}}\right)^{\frac{1}{2}}\left(\frac{T_{5,r}}{T_{3,r}}\right)^{\frac{1}{2}}\frac{P_{1,s}}{p_3}\frac{p_3}{P_{4,r}}\frac{P_{4,r}}{P_{5,r}}$$

where, from equation (9),

$$\frac{W\sqrt{\theta_{5,r}}}{\delta_{5,r}}=\frac{P_0}{\sqrt{T_0}}CA_5\sqrt{\frac{2\gamma g}{(\gamma-1)R}}X_{5,r}$$

Therefore, because $T_{3,r}=T_{5,r}$,

$$X_{5,r}=\frac{\dfrac{W\sqrt{\theta_{1,s}}}{\delta_{1,s}}\left(\dfrac{T_{3,r}}{T_{1,s}}\right)^{\frac{1}{2}}\dfrac{P_{1,s}}{p_3}\dfrac{p_3}{P_{4,r}}\dfrac{P_{4,r}}{P_{5,r}}}{\dfrac{P_0}{\sqrt{T_0}}CA_5\sqrt{\dfrac{2\gamma g}{(\gamma-1)R}}} \tag{20}$$

The only unknown quantity in the right-hand side of equation (20) is the pressure-loss term $P_{4,r}/P_{5,r}$ but in order to determine this term from the loss equation

$$\frac{P_{4,r}}{P_{5,r}}=\frac{b_5}{a_4}$$

b_5 must be known. The quantity b_5 is a function of $p_5/P_{5,r}$ and hence of X_5. A trial-and-error process must therefore be used.

A value of $p_5/P_{5,r}$ such that

$$\frac{p_3}{P_{4,r}}>\frac{p_5}{P_{5,r}}\geq\left(\frac{2}{\gamma+1}\right)^{\frac{\gamma}{\gamma-1}}$$

can be chosen as a first approximation. Then b_5, $P_{4,r}/P_{5,r}$, $X_{5,r}$, and finally $p_5/P_{5,r}$ can be obtained. From this second approximation, a second value of b_5 can be obtained and the process repeated. Convergence is rapid and the second approximation will usually be sufficiently accurate.

The maximum value that $X_{5,r}$ can have is the value that corresponds to sonic flow at the rotor exit, that is,

$$(X_{5,r})_{max}=\left[\left(\frac{2}{\gamma+1}\right)^{\frac{2}{\gamma-1}}-\left(\frac{2}{\gamma+1}\right)^{\frac{\gamma+1}{\gamma-1}}\right]^{\frac{1}{2}}$$

and if the value of $X_{5,r}$ from equation (20) is greater than this maximum, the values originally assumed for $p_3/P_{3,s}$ and

$U/\sqrt{\theta_{1,s}}$ must have been inadmissable. For each value of $U/\sqrt{\theta_{1,s}}$, a minimum value exists for $p_3/P_{3,s}$.

If the rotor is not choked, the static pressure in the annulus following the rotor p_6 is equal to the static pressure at the rotor throat p_5. When the rotor is choked, p_6 can be less than p_5 and consequently $p_6/P_{6,r}$ can be less than $p_5/P_{5,r}$. In this case a value can be assumed for $p_6/P_{6,r}$ and b_6 can be obtained from figure 2. This procedure can be summarized as follows: For the subcritical case,

$$X_5<\left[\left(\frac{2}{\gamma+1}\right)^{\frac{2}{\gamma-1}}-\left(\frac{2}{\gamma+1}\right)^{\frac{\gamma+1}{\gamma-1}}\right]^{\frac{1}{2}}$$

$$\frac{p_6}{P_{6,r}}=\frac{p_5}{P_{5,r}}$$

and

$$b_6=b_5$$

For the supercritical case,

$$X_5=\left[\left(\frac{2}{\gamma+1}\right)^{\frac{2}{\gamma-1}}-\left(\frac{2}{\gamma+1}\right)^{\frac{\gamma+1}{\gamma-1}}\right]^{\frac{1}{2}}$$

$$\frac{p_6}{P_{6,r}}\leq\frac{p_5}{P_{5,r}}$$

and

$$b_6\geq b_5$$

The velocity leaving the rotor with respect to the rotor is given by

$$\frac{V_{6,r}}{\sqrt{\theta_{3,r}}}=\sqrt{\frac{2\gamma gRT_0}{\gamma-1}}\left[1-\left(\frac{p_6}{P_{6,r}}\right)^{\frac{\gamma-1}{\gamma}}\right]^{\frac{1}{2}} \tag{21}$$

inasmuch as $T_{6,r}=T_{3,r}$.

The jet deflection at the rotor outlet ν_6 is obtained from figure 3 for $p_6/P_{6,s}$. The angle at which the fluid leaves the rotor is then

$$\sigma_f=\sigma-\nu_6 \tag{22}$$

From figure 5 the absolute velocity downstream of the rotor is

$$V_{6,s}=\sqrt{(V_{6,r}\sin\sigma_f-U)^2+(V_{6,r}\cos\sigma_f)^2}$$

or

$$V_{6,s}=V_{6,r}\sin\sigma_f[\cot^2\sigma_f+(1-r_o)^2]^{\frac{1}{2}} \tag{23}$$

where

$$r_o=\frac{U/\sqrt{\theta_{1,s}}}{(V_{6,r}/\sqrt{\theta_{1,s}})\sin\sigma_f} \tag{24}$$

The absolute exit angle ϵ can be obtained from

$$\tan\epsilon=\frac{V_{6,r}\sin\sigma_f-U}{V_{6,r}\cos\sigma_f}$$

or

$$\tan\epsilon=\tan\sigma_f(1-r_o) \tag{25}$$

The total temperature downstream of the rotor can be obtained by using equation (4) to give

$$T_{6,s}=t_6+\frac{(\gamma-1)V_{6,s}^2}{2\gamma gR}$$

and

$$T_{3,r}=T_{6,r}=t_6+\frac{(\gamma-1)V_{6,r}^2}{2\gamma gR}$$

or

$$T_{6,s}=T_{3,r}-\frac{(\gamma-1)(V_{6,r}^2-V_{6,s}^2)}{2\gamma gR}$$

Then from equations (23) and (24)

$$\frac{T_{6,s}}{T_{3,r}}=1-\frac{(\gamma-1)}{2\gamma gRT_0}\left(\frac{U}{\sqrt{\theta_{1,s}}}\right)^2\left(\frac{T_{1,s}}{T_{3,r}}\right)\left(\frac{2-r_o}{r_o}\right) \tag{26}$$

Because the tangential component of the velocity leaving the rotor is not generally converted into useful thrust, the total pressure downstream should be calculated from the axial component of the exit velocity; that is,

$$\frac{P_{6,s}}{p_6}=\left\{1+\frac{\gamma-1\left[\left(\frac{V_{6,r}}{\sqrt{\theta_{3,r}}}\right)\cos\sigma_f\right]^2}{2\gamma gRt_6T_0}\right\}^{\frac{\gamma}{\gamma-1}}$$

or, because

$$t_6=T_{3,r}\left[1-\frac{\gamma-1\left(\frac{V_{6,r}}{\sqrt{\theta_{3,r}}}\right)^2}{2\gamma gRT_0}\right]$$

$$\frac{P_{6,s}}{p_6}=\left\{\frac{1-\frac{\gamma-1}{2\gamma gRT_0}\left[\left(\frac{V_{6,r}}{\sqrt{\theta_{3,r}}}\right)\sin\sigma_f\right]^2}{1-\frac{\gamma-1}{2\gamma gRT_0}\left(\frac{V_{6,r}}{\sqrt{\theta_{3,r}}}\right)^2}\right\}^{\frac{\gamma}{\gamma-1}} \tag{27}$$

Performance parameters.—The fluid velocity, the pressure, and the temperature at any point in the turbine are now known. The turbine performance can be evaluated by combining these quantities to form the following parameters:

$$\frac{T_{6,s}}{T_{1,s}},\ \frac{p_6}{P_{1,s}},\ \frac{P_{6,s}}{P_{1,s}},\ \eta_{ad},\ \frac{\text{hp}}{\sqrt{\theta_{1,s}}\delta_{1,s}}$$

The ratio of total temperatures can be rewritten as

$$\frac{T_{6,s}}{T_{1,s}}=\left(\frac{T_{6,s}}{T_{3,r}}\right)\left(\frac{T_{3,r}}{T_{1,s}}\right)$$

or, with equations (26) and (18) as

$$\frac{T_{6,s}}{T_{1,s}}=\left[1-\frac{\gamma-1}{2\gamma gRT_0}\left(\frac{U}{\sqrt{\theta_{1,s}}}\right)^2\left(\frac{2-r_o}{r_o}\right)\left(\frac{T_{1,s}}{T_{3,r}}\right)\right]\left[1-\frac{\gamma-1}{2\gamma gRT_0}\left(\frac{U}{\sqrt{\theta_{1,s}}}\right)^2\left(\frac{2-r_i}{r_i}\right)\right]$$

Substitution for $T_{1,s}/T_{3,r}$ from equation (18) finally gives

$$\frac{T_{6,s}}{T_{1,s}}=1-\frac{\gamma-1}{2\gamma gRT_0}\left(\frac{U}{\sqrt{\theta_{1,s}}}\right)^2\left(\frac{2-r_i}{r_i}+\frac{2-r_o}{r_o}\right) \tag{28}$$

The other performance parameters can be obtained as follows:

$$\frac{p_6}{P_{1,s}}=\left(\frac{p_3}{P_{1,s}}\right)\left(\frac{P_{4,r}}{p_3}\right)\left(\frac{a_4}{b_6}\right)\left(\frac{p_6}{P_{6,r}}\right) \tag{29}$$

$$\frac{P_{6,s}}{P_{1,s}}=\left(\frac{p_6}{P_{1,s}}\right)\left(\frac{P_{6,s}}{p_6}\right) \tag{30}$$

$$\eta_{ad}=\frac{1-\frac{T_{6,s}}{T_{1,s}}}{1-\left(\frac{P_{6,s}}{P_{1,s}}\right)^{\frac{\gamma-1}{\gamma}}} \tag{31}$$

$$\text{hp}=\frac{\gamma}{\gamma-1}\,RT_{1,s}\left(1-\frac{T_{6,s}}{T_{1,s}}\right)W\left(\frac{1}{550}\right)$$

$$\frac{\text{hp}}{\sqrt{\theta_{1,s}}\,\delta_{1,s}}=\frac{\gamma T_0R}{(\gamma-1)550}\left(1-\frac{T_{6,s}}{T_{1,s}}\right)\frac{W\sqrt{\theta_{1,s}}}{\delta_{1,s}} \tag{32}$$

SUMMARY OF METHOD

Use of the method and of the results that can be obtained is exemplified by calculating the performance for the turbine of a commercial aircraft gas-turbine engine and by comparing the calculated with the experimental performance.

A summary of the method is as follows:

(a) Assume $p_3/P_{3,s}$ and $U/\sqrt{\theta_{1,s}}$.

(b) Find b_3 from figure 2 and ν_3 from figure 3.

(c) $\frac{p_3}{P_{1,s}}=\frac{p_3}{P_{3,s}}\left(\frac{1}{b_3}\right)$

(d) If $\frac{p_3}{P_{3,s}}\geq\left(\frac{2}{\gamma+1}\right)^{\frac{\gamma}{\gamma-1}}$, then $\frac{p_2}{P_{2,s}}=\frac{p_3}{P_{3,s}}$.

If $\frac{p_3}{P_{3,s}}<\left(\frac{2}{\gamma+1}\right)^{\frac{\gamma}{\gamma-1}}$, then $\frac{p_2}{P_{2,s}}=\left(\frac{2}{\gamma+1}\right)^{\frac{\gamma}{\gamma-1}}$.

(e) Find b_2 from figure 2.

(f) $X_{2,s}=\left[(p_2/P_{2,s})^{\frac{2}{\gamma}}-(p_2/P_{2,s})^{\frac{\gamma+1}{\gamma}}\right]^{\frac{1}{2}}$

(g) $$\frac{W\sqrt{\theta_{1,s}}}{\delta_{1,s}}=\frac{CA_2P_0}{\sqrt{T_0}\,b_2}\sqrt{\frac{2\gamma g}{(\gamma-1)R}}\left[\left(\frac{2}{\gamma+1}\right)^{\frac{2}{\gamma-1}}-\left(\frac{2}{\gamma+1}\right)^{\frac{\gamma+1}{\gamma-1}}\right]^{\frac{1}{2}} \tag{11}$$

(h) $$\frac{V_{3,s}}{\sqrt{\theta_{1,s}}}=\sqrt{T_0}\sqrt{\frac{2\gamma gR}{\gamma-1}}\left[1-\left(\frac{p_3}{P_{3,s}}\right)^{\frac{\gamma-1}{\gamma}}\right]^{\frac{1}{2}} \tag{13}$$

(i) $\alpha_{f,s}=\alpha-\nu_3$

(j) $$r_t=\frac{U/\sqrt{\theta_{1,s}}}{(V_{3,s}/\sqrt{\theta_{1,s}})\sin\alpha_{f,s}} \tag{14}$$

(k) $$\frac{V_{4,r}}{\sqrt{\theta_{1,s}}}=\frac{V_{3,s}}{\sqrt{\theta_{1,s}}}\cos\alpha_{f,s}\,[\cos\beta+(1-r_t)\tan\alpha_{f,s}\sin\beta] \tag{17}$$

(l) $$\frac{T_{3,r}}{T_{1,s}}=1-\frac{(\gamma-1)}{2\gamma gRT_0}\left(\frac{U}{\sqrt{\theta_{1,s}}}\right)^2\left(\frac{2-r_t}{r_t}\right) \tag{18}$$

(m) $$\frac{p_3}{P_{4,r}}=\left[1-\left(\frac{V_{4,r}}{\sqrt{\theta_{1,s}}}\right)^2\left(\frac{\sqrt{\theta_{1,s}}}{\sqrt{T_{3,r}}}\right)^2\frac{\gamma-1}{2\gamma gR}\right]^{\frac{\gamma}{\gamma-1}} \tag{19}$$

(n) Find a_4 from figure 2 and assume b_5.

(o) $$X_{5,r}=\frac{W\sqrt{\theta_{1,s}}}{\delta_{1,s}}\left(\frac{T_{3,r}}{T_{1,s}}\right)^{\frac{1}{2}}\left(\frac{P_{1,s}}{p_3}\right)\left(\frac{p_3}{P_{4,r}}\right)\left(a_4\right)\left(\frac{\sqrt{T_0}}{P_0}\right)\left[\frac{1}{CA_5\sqrt{\frac{2\gamma g}{(\gamma-1)R}}}\right]$$

(p) Find $p_5/P_{5,r}$ from figure 6.

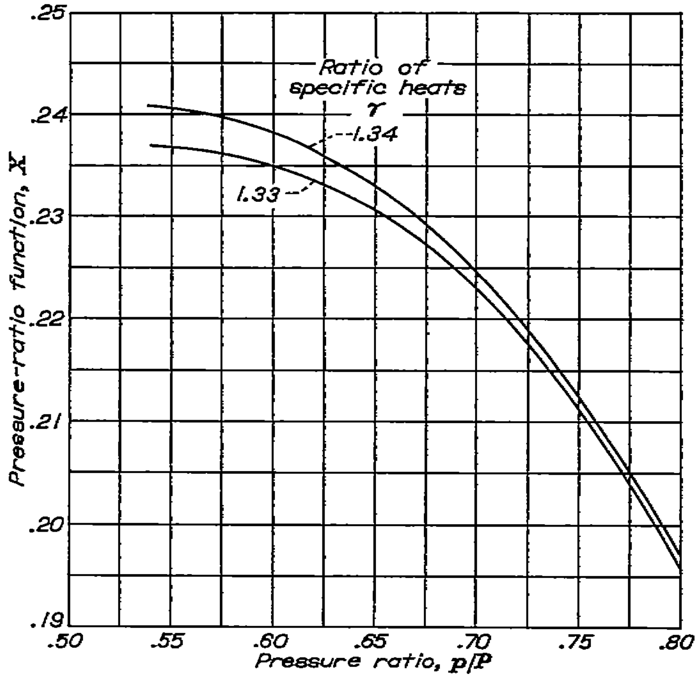

FIGURE 6.—Variation of pressure-ratio function with ratio of static to total pressure for two values of ratio of specific heats.

(q) Find b_5 from figure 2 and check with assumed b_5.

(r) If $\frac{p_5}{P_{5,r}}>\left(\frac{2}{\gamma+1}\right)^{\frac{\gamma}{\gamma-1}}$, then $\frac{p_6}{P_{6,r}}=\frac{p_5}{P_{5,r}}$.

If $\frac{p_5}{P_{5,r}}=\left(\frac{2}{\gamma+1}\right)^{\frac{\gamma}{\gamma-1}}$, assume $\frac{p_6}{P_{6,r}}\leq\left(\frac{2}{\gamma+1}\right)^{\frac{\gamma}{\gamma-1}}$.

(s) $$\frac{V_{6,r}}{\sqrt{\theta_{3,r}}}=\sqrt{\frac{2\gamma gRT_0}{\gamma-1}}\left[1-\left(\frac{p_6}{P_{6,r}}\right)^{\frac{\gamma-1}{\gamma}}\right]^{\frac{1}{2}} \tag{21}$$

(t) Find ν_6 from figure 3 and b_6 from figure 2.

(u) $$\sigma_f=\sigma-\nu_6 \tag{22}$$

(v) $$r_e=\frac{U/\sqrt{\theta_{1,s}}}{(V_{6,r}/\sqrt{\theta_{1,s}}\sin\sigma_f)} \tag{24}$$

(w) $$\frac{T_{6,s}}{T_{3,r}}=1-\left(\frac{\gamma-1}{2\gamma gRT_0}\right)\left(\frac{U}{\sqrt{\theta_{1,s}}}\right)^2\left(\frac{T_{1,s}}{T_{3,r}}\right)\left(\frac{2-r_e}{r_e}\right) \tag{26}$$

(x) $$\frac{P_{6,s}}{p_6}=\left\{\frac{1-\frac{\gamma-1}{2\gamma gRT_0}\left[\left(\frac{V_{6,r}}{\sqrt{\theta_{3,r}}}\right)\sin\sigma_f\right]^2}{1-\frac{\gamma-1}{2\gamma gRT_0}\left(\frac{V_{6,r}}{\sqrt{\theta_{3,r}}}\right)^2}\right\}^{\frac{\gamma}{\gamma-1}} \tag{27}$$

The performance parameters are:

$$\frac{T_{6,s}}{T_{1,s}}=1-\frac{\gamma-1}{2\gamma gRT_0}\left(\frac{U}{\sqrt{\theta_{1,s}}}\right)^2\left(\frac{2-r_t}{r_t}+\frac{2-r_e}{r_e}\right) \tag{28}$$

$$\frac{p_6}{P_{1,s}}=\left(\frac{p_3}{P_{1,s}}\right)\left(\frac{P_{4,r}}{p_3}\right)\left(\frac{a_4}{b_6}\right)\left(\frac{p_6}{P_{6,r}}\right) \tag{29}$$

$$\frac{P_{6,s}}{P_{1,s}}=\left(\frac{p_6}{P_{1,s}}\right)\left(\frac{P_{6,s}}{p_6}\right) \tag{30}$$

$$\eta_{ad}=\frac{1-\dfrac{T_{6,s}}{T_{1,s}}}{1-\left(\dfrac{P_{6,s}}{P_{1,s}}\right)^{\frac{\gamma-1}{\gamma}}} \tag{31}$$

$$\frac{\text{hp}}{\sqrt{\theta_{1,s}}\,\delta_{1,s}}=\frac{\gamma T_0 R}{(\gamma-1)550}\left(1-\frac{T_{6,s}}{T_{1,s}}\right)\frac{W\sqrt{\theta_{1,s}}}{\delta_{1,s}} \tag{32}$$

The geometrical properties of the turbine analyzed are:

$A_2=0.852$ square foot	$\alpha=62°$
$A_5=1.26$ square feet	$\beta=24°$
$D=1.833$ feet	$\sigma=47°$

The values of C, K, and γ for this example are assumed as follows:

$$C=0.98$$
$$K=0.30$$
$$\gamma_s=1.33$$
$$\gamma_r=1.34$$

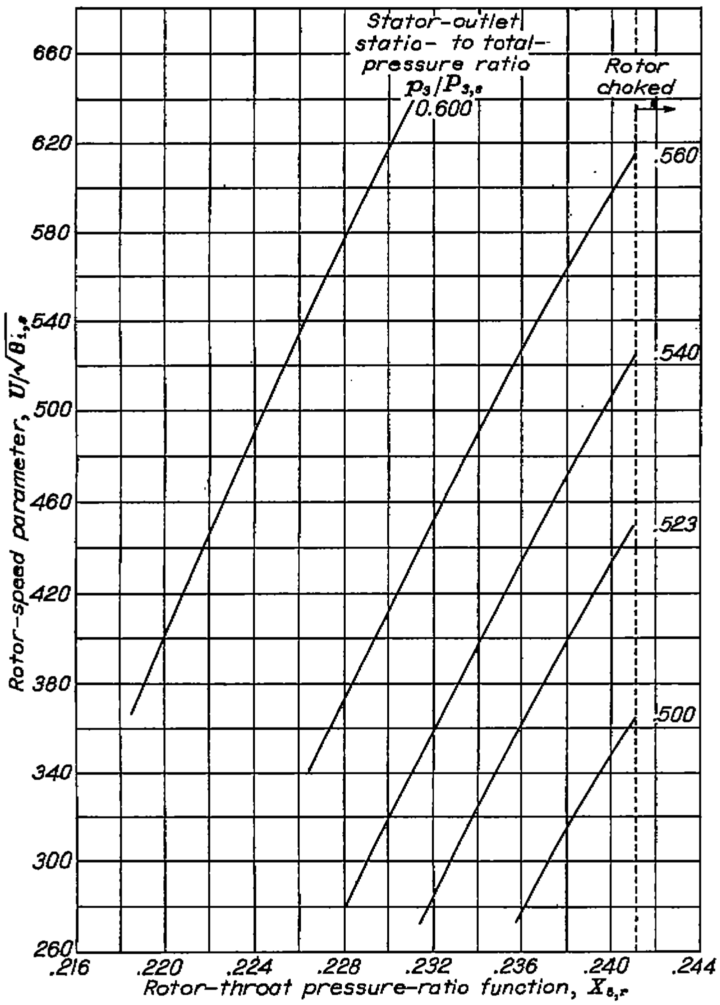

FIGURE 7.—Determination of rotor-speed parameter for which rotor-choking values occur at several values of ratio of static to total pressure at stator outlet. Turbine of typical example; K, 0.3; C, 0.98.

Sample calculations are given in table I.

For step (r), finding the value of $U/\sqrt{\theta_{1,s}}$ for which $p_5/P_{5,r}=0.537$ is necessary, that is, for which the rotor is choked and $X_{5,r}=0.241$. This value can be found most simply by plotting $X_{5,r}$ against $U/\sqrt{\theta_{1,s}}$ (fig. 7) and finding the value of $U/\sqrt{\theta_{1,s}}$ that corresponds to $X_{5,r}=0.241$.

Because the final dependent parameters are to be obtained as functions of $P_{1,s}/p_6$ for constant $U/\sqrt{\theta_{1,s}}$, having the choking values of $U/\sqrt{\theta_{1,s}}$ correspond to the initially chosen values of $U/\sqrt{\theta_{1,s}}$ is desirable. This correspondence can be accomplished by plotting the choking values of $U/\sqrt{\theta_{1,s}}$ against $p_3/P_{3,s}$ (fig. 8) and finding the values of $p_3/P_{3,s}$ that correspond to the desired values of $U/\sqrt{\theta_{1,s}}$.

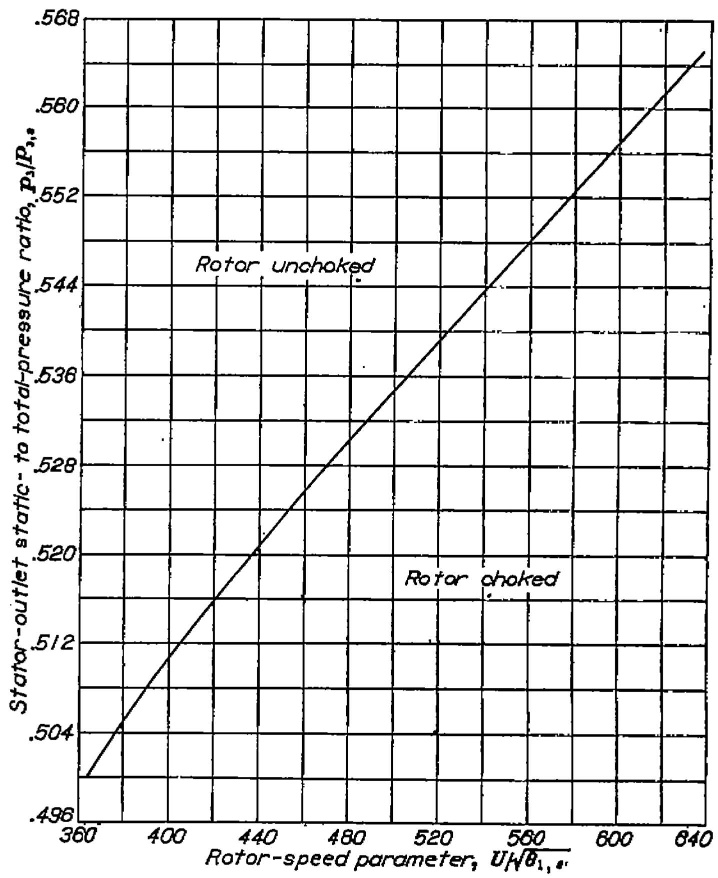

FIGURE 8.—Values of ratio of static to total pressure at stator outlet and rotor-speed parameter that correspond to rotor choking. Turbine of typical example; K, 0.3; C, 0.98.

From figure 8, the rotor-choking values of $p_3/P_{3,s}$ that correspond to values of $U/\sqrt{\theta_{1,s}}$ of 455 and 638 are 0.5245 and 0.5650, respectively. The performance calculations for these values of $p_3/P_{3,s}$ are summarized in table II.

The performance curves of figure 9 are plotted from the calculated values.

DISCUSSION OF PERFORMANCE CURVES

TRENDS OF CALCULATED PERFORMANCE

Choking of the turbine, in either the stator or the rotor, is one of the most important factors affecting turbine performance. The conditions for stator and rotor choking are obtained from table II for the turbine of the typical example and are given in figure 10. The turbine pressure ratio at which the stator chokes increases with increasing rotor-speed parameter, whereas the pressure ratio for rotor choking is almost independent of the speed parameter. For values of the rotor-speed parameter greater than 525, the stator cannot choke because choking has already occurred in the rotor.

Another important consideration is the variation of inlet and outlet velocity ratios. These ratios determine the rotor entry- and exit-whirl losses and affect mainly the adiabatic efficiency. When the fluid enters the rotor at the blade-entrance angle, the inlet velocity ratio from equation (17) is

$$r_i = 1 - \frac{\tan 24^\circ}{\tan 62^\circ} = 0.763$$

For axial outlet velocity (that is, no whirl), the outlet velocity ratio r_e is equal to 1.00. As shown in figure 11, the speed parameter and pressure ratio for which both of these conditions are satisfied are 638 and 2.55, respectively.

The variation of the temperature-ratio parameter with turbine pressure ratio is shown in figure 9 (a). The temperature-ratio parameter is directly proportional to the change of the whirl component of the fluid as it passes through the rotor. For turbine pressure ratios less than the pressure

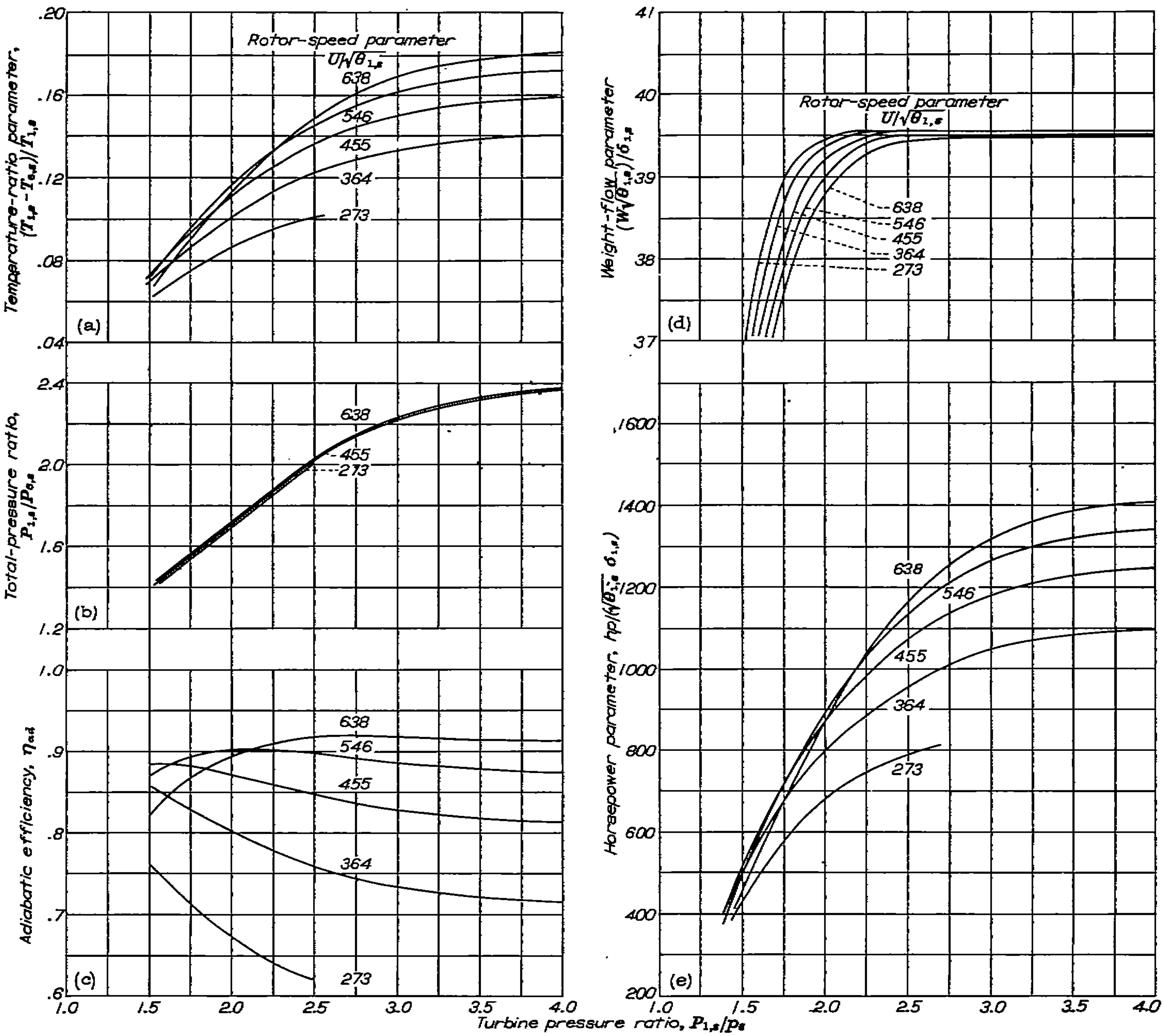

(a) Temperature-ratio parameter.
(b) Total-pressure ratio.
(c) Adiabatic efficiency.
(d) Weight-flow parameter.
(e) Horsepower parameter.

FIGURE 9.—Dependent parameters for turbine of typical example

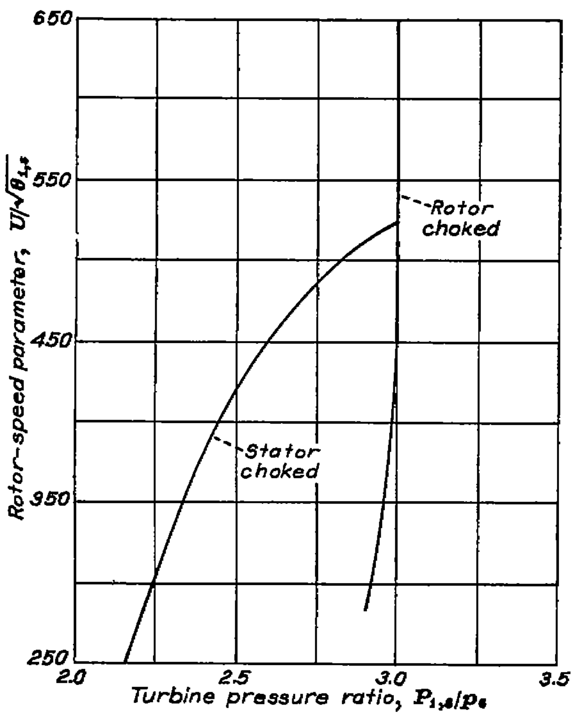

FIGURE 10.—Conditions for turbine choking in turbine of typical example. K, 0.3; C, 0.98.

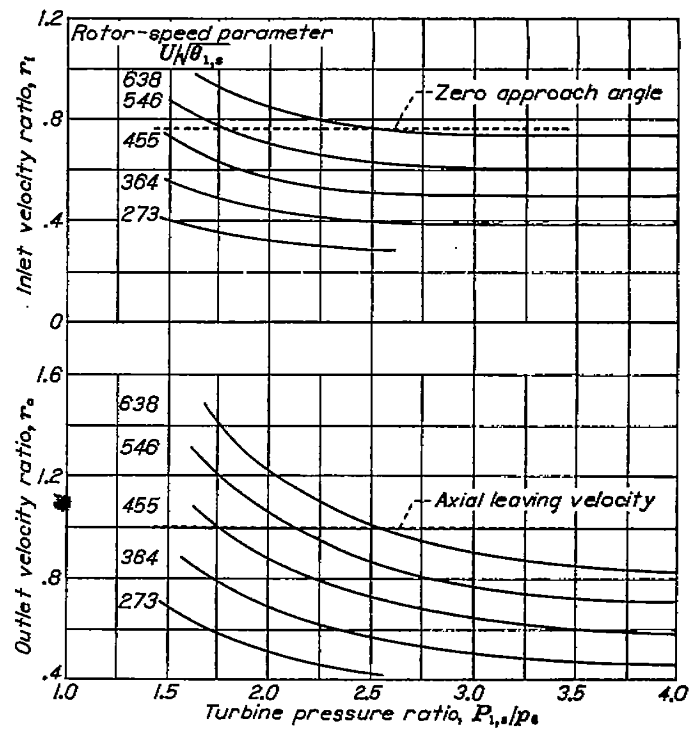

FIGURE 11.—Variation of inlet and outlet velocity ratios for turbine of typical example. K, 0.3; C, 0.98.

ratio for rotor choking (fig. 10), both the entering and leaving whirl components increase with pressure ratio. For turbine pressure ratios greater than the rotor-choking pressure ratio, however, the entering whirl component is constant and, because of the jet deflection, the leaving whirl component is maintained almost constant even though the exit velocity increases with increasing pressure ratio. Hence for any given rotor-speed parameter, the temperature-ratio parameter increases with increasing turbine pressure ratio until the rotor chokes. At pressure ratios higher than choking, the temperature-ratio parameter remains relatively constant.

The total-pressure ratio (fig. 9 (b)) is a function mainly of the turbine pressure ratio, the rotor-speed parameter having a very small effect. It should be remembered that for this analysis the downstream total pressure $P_{6,s}$ has been obtained from the axial component on the downstream velocity rather than the total downstream velocity.

The adiabatic efficiency given in figure 9 (c) is also dependent on the definition of downstream total pressure. The greatest efficiency is obtained for a speed parameter of 638 and a pressure ratio of approximately 2.55, which is in accordance with the previous discussion of the effect of the velocity ratios on adiabatic efficiency.

The weight-flow parameter (fig. 9 (d)) increases with turbine pressure ratio until the turbine chokes, and then remains constant. For the two highest speed parameters (638 and 546), the weight flow is limited by rotor choking, whereas for lower speed parameters the weight flow is limited by stator choking. The greatest weight flow is slightly less for rotor-choking speed parameters than for stator-choking speed parameters.

The variation of the horsepower parameter is shown in figure 9 (e). The horsepower parameter is proportional to the product of the temperature-ratio parameter and the weight-flow parameter, both of which increase with turbine pressure ratio for pressure ratios less than 2. For pressure ratios between 2 and 3, the temperature-ratio parameter continues to increase but the weight-flow parameter is almost constant so that the horsepower parameter continues to increase, though not so rapidly as for pressure ratios less than 2. For pressure ratios greater than 3, the weight-flow parameter is constant, the temperature-ratio parameter is almost constant, and the horsepower parameter is almost constant.

The effect of the choice of the blading-loss parameter on the dependent parameters is shown in figure 12. The effect can be seen to consist mainly of a vertical shifting of the curves, each curve retaining its general shape independently of the blading-loss parameter. For a given turbine pressure ratio, increasing the blading-loss parameter by 0.1 results in an increase in the total-pressure ratio of approximately 0.5 percent and a decrease in the temperature-ratio parameter and the adiabatic efficiency of approximately 2.0 percent.

COMPARISON WITH EXPERIMENTAL RESULTS

The turbine of the typical example has been operated at the NACA Lewis laboratory as a part of a gas-turbine engine and the resulting data have been used to obtain the turbine performance parameters. The variation of temperature-ratio parameter and adiabatic efficiency with rotor-speed parameter is presented in figure 13 for values of the turbine total-pressure ratio ranging from 1.71 to 2.34. Curves of calculated performance are also presented for values of the blading-loss parameter of 0.3 and 0.5. In general, the temperature-ratio-parameter comparison indicates a blading-loss parameter of about 0.3 except at a pressure ratio of 2.34 where the blading-loss parameter shows some increase. The trend of the efficiency comparison is toward a blading-loss parameter somewhat higher than 0.3, but in general less

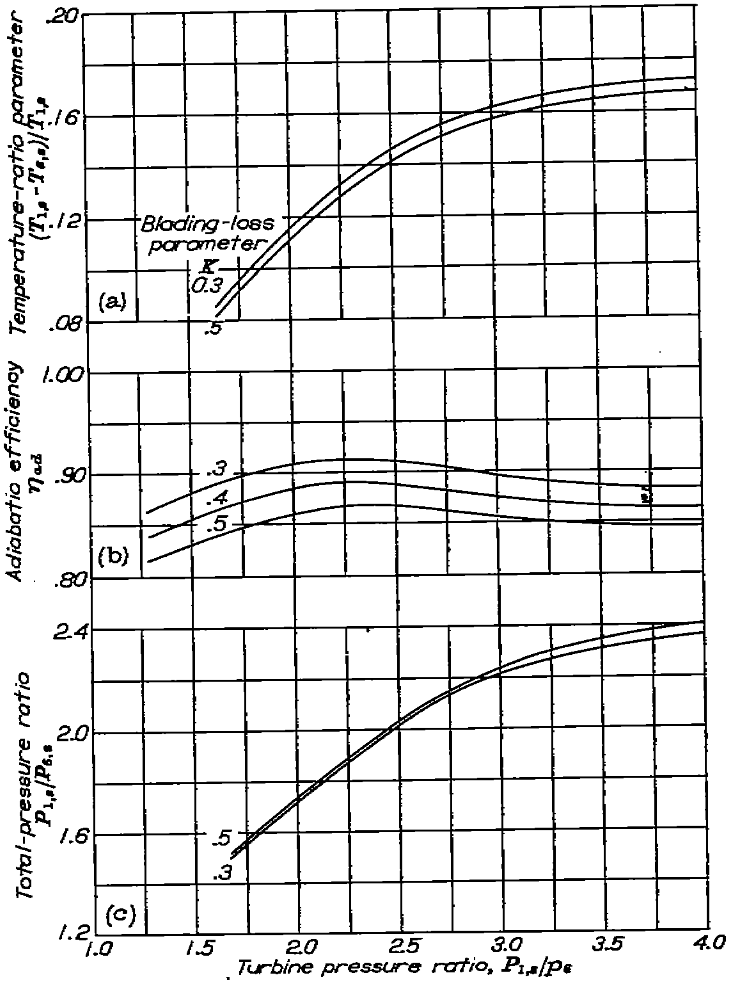

(a) Temperature-ratio parameter.
(b) Adiabatic efficiency.
(c) Total-pressure ratio.

FIGURE 12.—Effect of blading-loss parameter on dependent parameters. Turbine of typical example; $U/\sqrt{\theta_{1,s}}$, 546; C, 0.98.

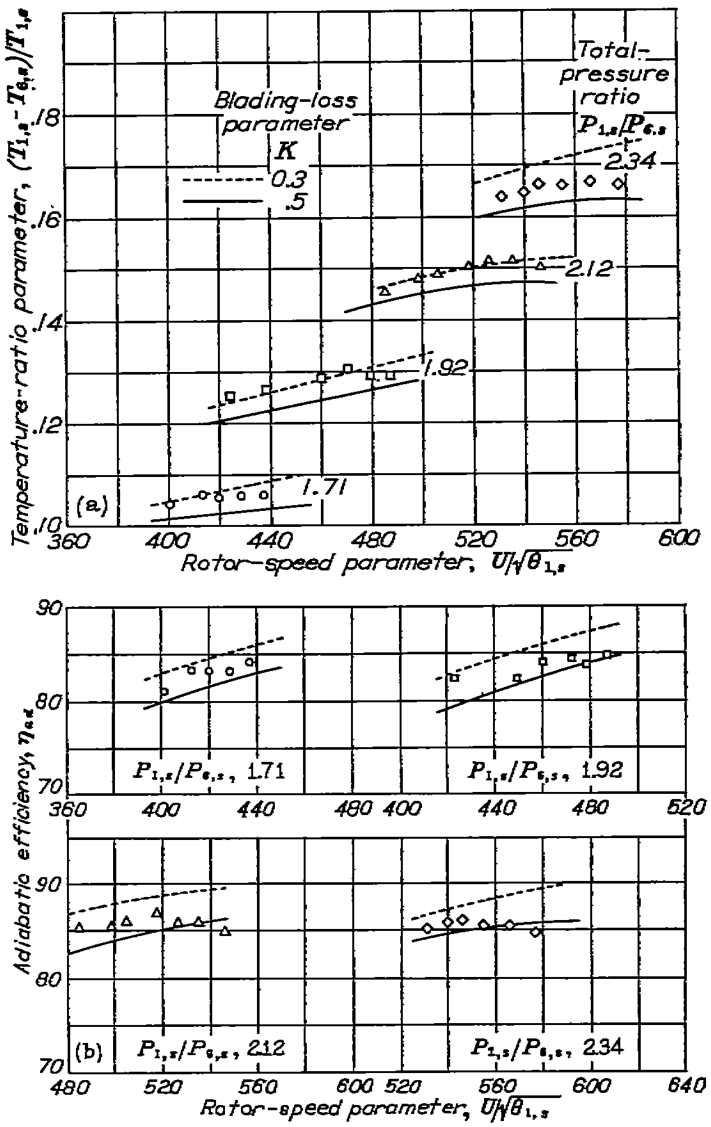

(a) Variation of temperature-ratio parameter with rotor-speed parameter.
(b) Variation of adiabatic efficiency with rotor-speed parameter.

FIGURE 13.—Comparison between theoretical and experimental results for turbine of typical example.

than 0.5. The trend of a higher indicated blading-loss parameter on the basis of the efficiency comparison is probably due to the additional error involved in the use of an experimentally determined pressure ratio to calculate the measured efficiency. The importance of additional investigations of conditions that influence the blading-loss parameter is clearly evident inasmuch as the degree of agreement between theory and experiment is contingent on the proper choice of this parameter. For the turbine investigated, a blading-loss parameter of 0.5 would be slightly higher than the experiments indicate and the complete engine would actually perform somewhat better than would be predicted by a theoretical-matching study.

SUMMARY OF RESULTS

From a theoretical investigation of the performance of the turbine component of a commercial aircraft gas-turbine engine and a comparison of the performance calculated by means of the analytical method and the experimental performance, the following results are indicated:

1. For the turbine of the typical example, the assumed pressure losses and turning angles give a calculated performance that represents the trends of the experimental performance with reasonable accuracy.

2. The agreement between analytical performance and experimental performance is contingent upon the proper selection of blading-loss parameter. The experimental data indicate that for the turbine of the typical example the blading-loss parameter varied from 0.3 to 0.5 for most of the range investigated.

3. The methods of analysis should be applicable to any turbine with reasonably well-designed blading, although the same coefficient will not necessarily apply. For turbines with poor blading design, the pressure losses and the turning angles will be difficult to evaluate and the trends, as well as the magnitudes of the calculated performance, may be incorrect.

LEWIS FLIGHT PROPULSION LABORATORY,
NATIONAL ADVISORY COMMITTEE FOR AERONAUTICS,
CLEVELAND, OHIO, *December 29, 1948.*

APPENDIX A

BLADE FRICTION LOSSES

The loss in total pressure due to friction effects that occur when a fluid passes through a cascade depends on the design of the particular cascade, on the Reynolds number, and on the average dynamic head in the cascade. For a particular cascade, however, the effect of a change in the Reynolds number caused by a change in operating conditions should be small even for a reasonably wide range of operating conditions. The loss can therefore be approximated by

$$\Delta P_{loss}=\frac{2(\gamma-1)}{\gamma}K\left(\frac{1}{2}\rho V^2\right) \tag{33}$$

where K is a constant for the particular cascade and $\frac{1}{2}\rho V^2$ is the average dynamic head in the cascade.

From equations (5), (6), and (7),

$$\frac{1}{2}\rho V^2=\frac{\gamma}{\gamma-1}P\left[1-\left(\frac{p}{P}\right)^{\frac{\gamma-1}{\gamma}}\right]\left(\frac{p}{P}\right)^{\frac{1}{\gamma}}$$

The average dynamic head in the cascade of figure 1 is then approximately

$$\frac{\gamma}{2(\gamma-1)}\left\{P_b\left(\frac{p_b}{P_b}\right)^{\frac{1}{\gamma}}\left[1-\left(\frac{p_b}{P_b}\right)^{\frac{\gamma-1}{\gamma}}\right]+P_c\left(\frac{p_c}{P_c}\right)^{\frac{1}{\gamma}}\left[1-\left(\frac{p_c}{P_c}\right)^{\frac{\gamma-1}{\gamma}}\right]\right\} \tag{34}$$

The pressure loss then becomes

$$\Delta P_{loss}=P_b-P_c$$
$$=K\left\{P_b\left(\frac{p_b}{P_b}\right)^{\frac{1}{\gamma}}\left[1-\left(\frac{p_b}{P_b}\right)^{\frac{\gamma-1}{\gamma}}\right]+P_c\left(\frac{p_c}{P_c}\right)^{\frac{1}{\gamma}}\left[1-\left(\frac{p_c}{P_c}\right)^{\frac{\gamma-1}{\gamma}}\right]\right\}$$

or

$$P_b a=P_c b \tag{35}$$

where

$$\left.\begin{aligned} a&=1-K\left(\frac{p_b}{P_b}\right)^{\frac{1}{\gamma}}\left[1-\left(\frac{p_b}{P_b}\right)^{\frac{\gamma-1}{\gamma}}\right]\\ b&=1+K\left(\frac{p_c}{P_c}\right)^{\frac{1}{\gamma}}\left[1-\left(\frac{p_c}{P_c}\right)^{\frac{\gamma-1}{\gamma}}\right]\end{aligned}\right\} \tag{36}$$

The variation of the blading-loss functions with the ratio of static to total pressure for several values of blading-loss parameter is shown in figure 2.

For the stator the entrance velocity is small; then

$$a\approx 1$$

and equation (35) becomes

$$P_{1,s}=P_{3,s}b_3$$

For the rotor, equation (35) becomes

$$P_{4,r}a_4=P_{6,r}b_6$$

APPENDIX B

JET DEFLECTION

The expansion of a uniform two-dimensional frictionless stream of gas flowing around a corner at sonic or supersonic speeds has been investigated by Prandtl and Meyer. The analysis of reference 6 shows that the jet deflection is given by

$$\nu=x-y \tag{37}$$

$$\left(\frac{p}{P}\right)^{\frac{\gamma-1}{\gamma}}=\frac{1}{\gamma+1}\left(1+\cos 2\sqrt{\frac{\gamma-1}{\gamma+1}}\,x\right) \tag{38}$$

$$\tan y=\sqrt{\frac{\gamma+1}{\gamma-1}}\tan\left(\sqrt{\frac{\gamma-1}{\gamma+1}}\,x\right) \tag{39}$$

where ν is the angle of jet deflection and p/P is the ratio of static to total pressure in the region beyond the trailing edge. For the purpose of this discussion, x and y can be regarded as jet-deflection parameters. A value is assumed for x, the pressure ratio p/P and y are computed from equations (38) and (39), respectively, and ν is obtained from equation (37). Then ν is known as a function of p/P. (See fig. 3.)

REFERENCES

1. Morley, A. W.: Equilibrium Running of the Simple Jet-Turbine Engine. R. A. S. Jour., vol. 52, no. 449, May 1948, pp. 305–322.
2. Goldstein, Arthur W.: Analysis of the Performance of a Jet Engine from Characteristics of the Components. I—Aerodynamic and Matching Characteristics of the Turbine Component Determined with Cold Air. NACA Rep. 878, 1947.
3. Stodola, A.: Steam and Gas Turbines. Vol. 1. McGraw-Hill Book Co., Inc., 1927, pp. 256–286. (Reprinted, Peter Smith (New York), 1945.)
4. Harris, R. G., and Fairthorne, R. A.: Wind Tunnel Experiments with Infinite Cascades of Aerofoils. R. & M. No. 1206, British A. R. C., 1928.
5. Kantrowitz, Arthur, and Erwin, John R.: Cascade Investigation of Buckets for a Modern Aircraft Turbosupercharger. NACA ACR L4J25, 1944.
6. Taylor, G. I., and Maccoll, J. W.: The Mechanics of Compressible Fluids. Vol. III, div. H of Aerodynamic Theory, W. F. Durand, ed., Julius Springer (Berlin), 1935, pp. 243–246.

TABLE I.—SAMPLE CALCULATIONS FOR UNCHOKED TURBINE ROTOR OF TYPICAL EXAMPLE

[K, 0.3; C, 0.98]

$\frac{p_2}{P_{1,x}}$	$\frac{p_3}{P_{1,x}}$	$\frac{W\sqrt{\theta_{1,x}}}{\delta_{1,x}}$	$\frac{V_{3,x}}{\sqrt{T_{1,x}}}$	$\alpha_{f,x}$	$\frac{U}{\sqrt{\theta_{1,x}}}$	r_i	$\frac{T_{3,r}}{T_{1,x}}$	$\frac{p_3}{P_{3,r}}$	$\frac{p_5}{P_{3,r}}$	$\frac{p_6}{P_{3,r}}$	$\frac{P_{6,r}}{P_{3,r}}$	$\frac{V_{6,x}}{\sqrt{T_{3,r}}}$	r_e	$\frac{T_{6,x}}{T_{1,x}}$	$\frac{P_{6,x}}{p_6}$	$\frac{P_{1,x}}{p_6}$	$\frac{P_{1,x}}{P_{6,x}}$	η_{ad}	$\frac{hp}{\delta_{1,x}\sqrt{\theta_{1,x}}}$
0.600	0.5854	39.36	40.58	62.0	273.2 455.4 637.6	0.3349 .5582 .7815	0.9471 .9236 .9096	0.7967 .8358 .8737	0.740 .709 .664	0.740 .709 .664	0.9680 .9685 .9685	31.55 33.65 36.56	0.5343 .8456 1.0980	0.9179 .8833 .8620	1.153 1.178 1.217	1.900 2.078 2.319	1.646 1.764 1.906	0.689 .870 .913	607.8 864.2 1021.8
0.560	0.5455	39.52	43.06	62.0	455.4 614.8	0.5260 .7107	0.9171 .9021	0.8089 .8437	0.654 .537	0.654 .537	0.9645 .9620	37.18 44.45	0.7679 .8743	0.8697 .8326	1.225 1.352	2.350 2.993	1.919 2.215	0.853 .914	968.8 1243.6
0.540	0.5258	39.54	44.27	62.0	273.2 455.4 523.7	0.3070 .5116 .5884	0.9413 .9140 .9062	0.7538 .7948 .8103	0.682 .608 .537	0.682 .608 .537	0.9620 .9620 .9590	35.39 40.06 44.45	0.4778 .7141 .7431	0.9074 .8607 .8401	1.200 1.270 1.352	2.182 2.581 2.990	1.819 2.065 2.212	0.652 .844 .875	688.8 1036.3 1190.1
0.523	0.5068	39.54	45.34	61.8	273.2 448.6	0.3003 .4930	0.9398 .9123	0.7395 .7795	0.660 .537	0.660 .537	0.9610 .9585	36.81 44.45	0.4598 .6344	0.9041 .8505	1.219 1.352	2.290 2.979	1.877 2.201	0.648 .822	713.4 1112.0
0.500	0.4859	39.54	46.74	61.3	273.2 364.3	0.2927 .3902	0.9379 .9219	0.7184 .7392	0.621 .537	0.621 .537	0.9590 .9562	39.29 44.45	0.4312 .5125	0.8992 .8670	1.241 1.352	2.484 2.962	2.001 2.191	0.623 .736	750.0 958.6

TABLE II.—SAMPLE CALCULATIONS FOR CHOKED TURBINE ROTOR OF TYPICAL EXAMPLE

[K, 0.3; C, 0.98]

$\frac{p_2}{P_{1,x}}$	$\frac{p_3}{P_{1,x}}$	$\frac{W\sqrt{\theta_{1,x}}}{\delta_{1,x}}$	$\frac{V_{3,x}}{\sqrt{T_{1,x}}}$	$\alpha_{f,x}$	$\frac{U}{\sqrt{\theta_{1,x}}}$	r_i	$\frac{T_{3,r}}{T_{1,x}}$	$\frac{p_3}{P_{3,r}}$	$\frac{p_5}{P_{3,r}}$	$\frac{p_6}{P_{6,r}}$	$\frac{P_{6,r}}{P_{3,r}}$	$\frac{V_{6,x}}{\sqrt{T_{3,r}}}$	r_e	$\frac{T_{6,x}}{T_{1,x}}$	$\frac{P_{6,x}}{p_6}$	$\frac{P_{1,x}}{p_6}$	$\frac{P_{1,x}}{P_{6,x}}$	η_{ad}	$\frac{hp}{\delta_{1,x}\sqrt{\theta_{1,x}}}$
0.5650	0.5506	39.49	42.74	62.0	637.6	0.7420	0.9017	0.8523	0.537	0.537 .500 .450 .400	0.9625 .9610 .9600 .9590	44.46 46.73 49.83 53.00	0.9069 .8727 .8441 .8282	0.8319 .8269 .8224 .8198	1.3514 1.4131 1.5311 1.6966	2.996 3.220 3.531 4.038	2.214 2.280 2.340 2.379	0.9185 .9169 .9143 .9125	1314.4 1353.5 1388.6 1409.4
0.5245	0.5103	39.54	45.23	61.8	455.4	0.5017	0.9117	0.7822	0.537	0.537 .500 .450 .400	0.9625 .9610 .9600 .9590	44.46 46.73 49.83 53.00	0.6442 .6200 .5997 .5883	0.8495 .8459 .8427 .8408	1.3514 1.4131 1.5311 1.6966	2.960 3.200 3.565 4.012	2.203 2.266 2.328 2.366	0.8278 .8214 .8150 .8109	1177.0 1205.0 1230.5 1245.0